

See discussions, stats, and author profiles for this publication at: <https://www.researchgate.net/publication/200655779>

# Efficacy of Au–Au Contacts for Scanning Tunneling Microscopy Molecular Conductance Measurements

ARTICLE *in* THE JOURNAL OF PHYSICAL CHEMISTRY C · NOVEMBER 2007

Impact Factor: 4.77 · DOI: 10.1021/jp0756101

---

CITATIONS

10

---

READS

12

3 AUTHORS, INCLUDING:



Latha Venkataraman

Columbia University

116 PUBLICATIONS 4,426 CITATIONS

SEE PROFILE

# Efficacy of Au–Au Contacts for Scanning Tunneling Microscopy Molecular Conductance Measurements

David Millar,<sup>‡</sup> Latha Venkataraman,<sup>§</sup> and Linda H. Doerr<sup>\*,†</sup>

Chemistry Department, Boston University, 590 Commonwealth Avenue, Boston, Massachusetts 02215, Department of Chemistry, Barnard College, 3009 Broadway, New York, New York 10027, and Department of Applied Physics and Applied Mathematics and Center for Electron Transport in Molecular Nanostructures, Columbia University, New York, New York 10027

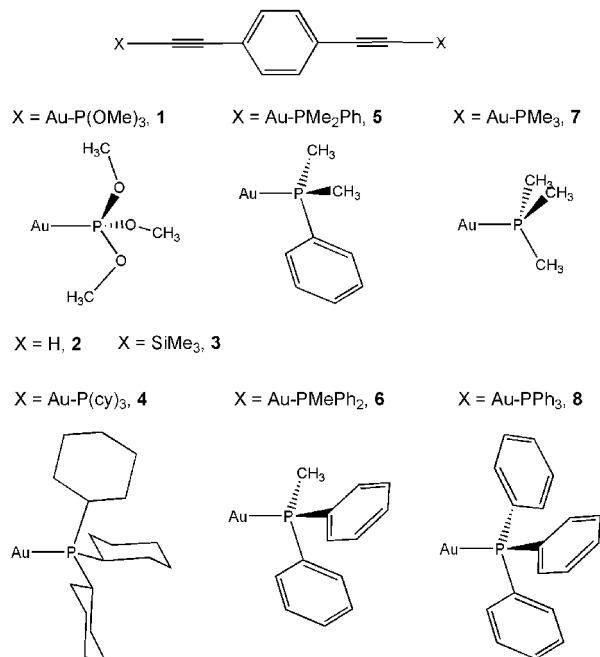
Received: July 17, 2007; In Final Form: September 1, 2007

We measured conductance traces while breaking gold point contacts in a solution of molecules containing the  $\mu$ -*p*-phenylenediethynyl  $X-C\equiv C-C_6H_4-C\equiv C-X$  unit, with eight different capping X groups: Au–P(OMe)<sub>3</sub> (**1**), H (**2**), SiMe<sub>3</sub> (**3**), Au–P(cy)<sub>3</sub> (**4**), Au–PMe<sub>2</sub>Ph (**5**), Au–PMePh<sub>2</sub> (**6**), Au–PMe<sub>3</sub> (**7**), and Au–PPh<sub>3</sub> (**8**). Our goal with this work was to achieve a direct Au–C link with a conjugated organic group, potentially forming a molecular junction without chemical link groups that typically decrease junction conductances, such as thiols or amines. Conductance traces collected in the presence of molecules **1**, **2**, **3**, **5**, and **7** reveal additional steps at conductances as high as 0.1  $G_0$  ( $G_0 = 2e^2/h$ ) down to the measurable limits of the experimental setup. Conductance histograms generated from these traces therefore show a broad increase of counts when compared to a control histogram collected in the solvent alone suggesting the binding of the molecules to the broken Au contacts. The histograms for molecules **1**, **5**, **7**, and **2** were not distinguishable, although that of molecule **3** had considerably fewer counts over the entire conductance range, suggesting that the steric bulk of the SiMe<sub>3</sub> prevented frequent junction formation. The histograms collected in a solution of molecules **4**, **6**, or **8** did not differ from that of the control histogram probably because of the steric bulk of the Au–PR<sub>3</sub> capping groups prevented the formation a molecular junction.

In the development of components for molecular electronics, the conductance properties of candidate wires (molecules) must be measured and compared.<sup>1,2</sup> The most widely used bonding strategy to attach molecules covalently to gold electrodes is reaction of dithiols<sup>3–10</sup> directly with gold. Dithiol compounds have been studied extensively using a plethora of methods,<sup>3,4,9,11–15</sup> but it is well-known that the Au–S link, which involves a covalent  $\sigma$  bond, does not provide a high conductance link between the molecule and the electrodes. Recent work using amine linkages to gold (Au–N) provides clear statistical signatures for single-molecule conductance,<sup>15,16</sup> however, the contact resistance of these linkages is still high. Therefore, new types of metal(electrode)–molecule (M–X) junctions are of interest in order to provide good energy alignment between electrode and molecule.<sup>17</sup> Direct metal surface to carbon double bonds have been prepared in ruthenium–carbene (Ru=C)<sup>18</sup> and molybdenum carbide–carbene (Mo=C)<sup>19</sup> systems. In the former case, theoretical and experimental work suggest that the conductance through the link could provide a resonant tunneling scenario.<sup>18</sup>

In this work, we explore the possibility of making a direct contact between a gold metal atom and a carbon atom on both ends of a molecule. We have chosen to investigate the conductance of compounds that have an extended conjugated  $\pi$ -system ( $X-C\equiv C-C_6H_4-C\equiv C-X$ ) with eight different capping X groups as shown in Scheme 1: Au P(OMe)<sub>3</sub> (**1**), H (**2**), SiMe<sub>3</sub> (**3**), Au P(cy)<sub>3</sub> (**4**), Au–PMe<sub>2</sub>Ph (**5**), Au–PMePh<sub>2</sub> (**6**),

**SCHEME 1: End Capping Groups of C<sub>10</sub>H<sub>4</sub> *p*-Phenyldiacteylene Fragment**



Au–PMe<sub>3</sub> (**7**), and Au–PPh<sub>3</sub> (**8**). The {Au<sub>2</sub>C<sub>10</sub>H<sub>4</sub>} unit is electrostatically neutral and exists as a pure compound<sup>20</sup> but is insoluble due to extensive cross-linking of the electron-deficient gold atoms to the C≡C bonds in adjacent molecules. It has been established that efficient electronic conduction is facilitated by

\* Corresponding author. E-mail: doerr@bu.edu.

<sup>†</sup> Boston University.

<sup>‡</sup> Barnard College.

<sup>§</sup> Columbia University.

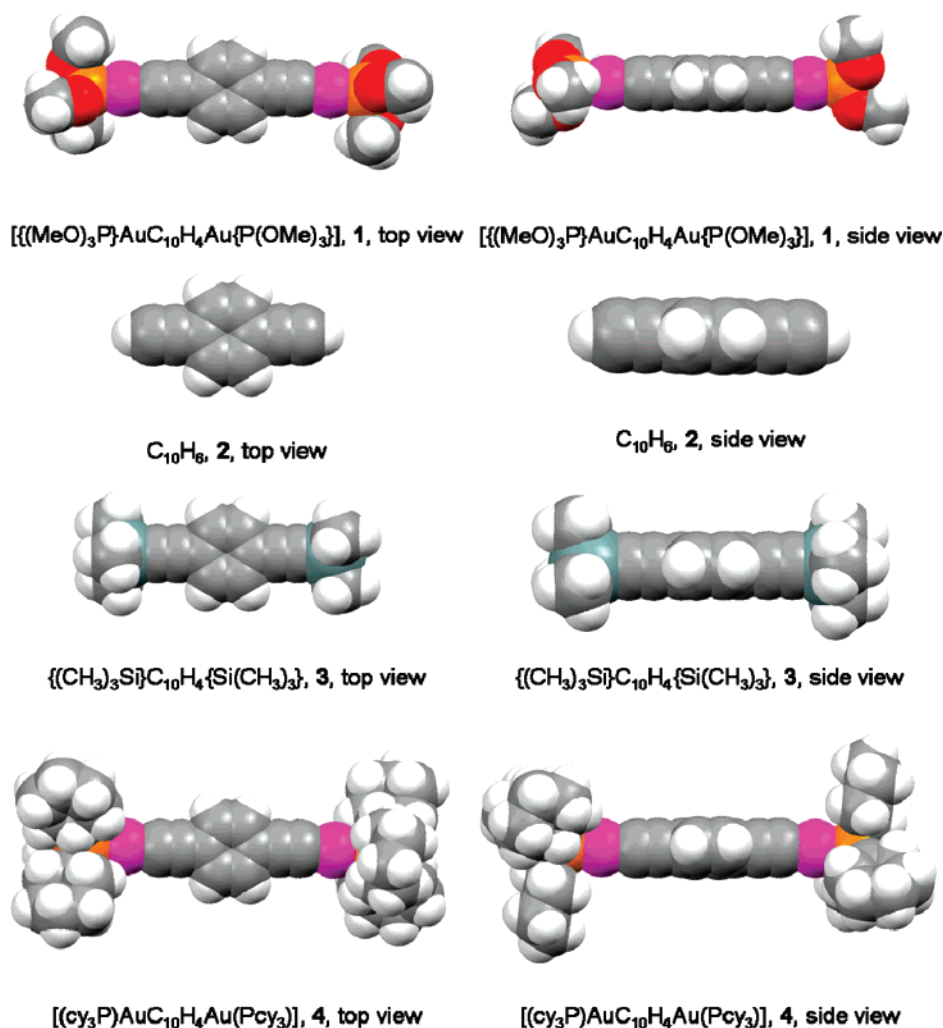
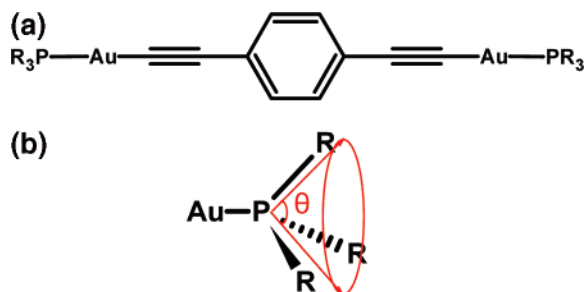


Figure 1. Space-filling models based on crystallographic data of compounds **1**, **2**, **3**, and **4**.

SCHEME 2: (a)  $\mu$ -*p*-Phenylenediethynyl-bis[(PR<sub>3</sub>)gold(I)] and (b) Cone Angle,  $\theta$



(i) delocalized systems of  $\pi$ -symmetry<sup>21</sup> and (ii) orbital energy matching between atoms in the contacts<sup>22</sup> and atoms in the conducting molecule. The capping X groups on the terminal carbons have different sizes, as shown in Figure 1, thus changing the accessibility of the terminal acetylide C to the Au atoms on the electrodes and leading to possible variations in measured conductance traces. In addition, for molecules **1** and **4**, there is a possibility that the Au atoms on the electrodes bind to the Au atoms in the molecule.

Reaction of the {Au<sub>2</sub>C<sub>10</sub>H<sub>4</sub>}<sub>∞</sub> polymer with neutral phosphines and phosphites, PR<sub>3</sub>, readily forms soluble compounds that contain the conducting organic moiety and have linearly coordinated gold atoms as shown in Scheme 2a. These gold atoms are not coordinatively saturated and can bond further, and they do so most often with other gold atoms. Driven by

TABLE 1: Cone Angle of Selected Phosphorus Ligands with Increasing Steric Bulk in the LAuC<sub>10</sub>H<sub>4</sub>AuL Family<sup>a</sup>

compd	L	cone angle, $\theta$ (deg)
<b>1</b>	P(OMe) <sub>3</sub>	107
<b>4</b>	Pcy <sub>3</sub>	179
<b>5</b>	P(Me) <sub>2</sub> Ph	127
<b>6</b>	PMe(Ph) <sub>2</sub>	136
<b>7</b>	P(Me) <sub>3</sub>	118
<b>8</b>	PPh <sub>3</sub>	145

<sup>a</sup> Ref 28.

dispersion or electron correlation effects, two gold atoms interact at a distance of less than the sum of their van der Waals radii (ca. 3.6 Å)<sup>23</sup> with structurally characterized examples exhibiting Au...Au contacts in the range of 2.8–3.3 Å. The energies of these interactions have been estimated<sup>24</sup> theoretically to be 5–15 kcal/dimer which are comparable to those of hydrogen bonding.<sup>25,26</sup>

Previous structural characterization of compounds **1** and **7** demonstrated Au...Au contacts of 3.1722(3)<sup>27</sup> and 3.1369(1) Å,<sup>20</sup> respectively. These two compounds have phosphorus groups with the smallest cone angles,  $\theta$ , which are defined by the van der Waals surface of the ligands from CPK models, Scheme 2b.<sup>28</sup> The cone angles for the phosphine and phosphite groups used in this study are collected in Table 1. Compounds **4**, **6**, and **8** contain significantly larger {(R<sub>3</sub>P)Au} groups such that **4** did not exhibit any close Au...Au contacts in the solid

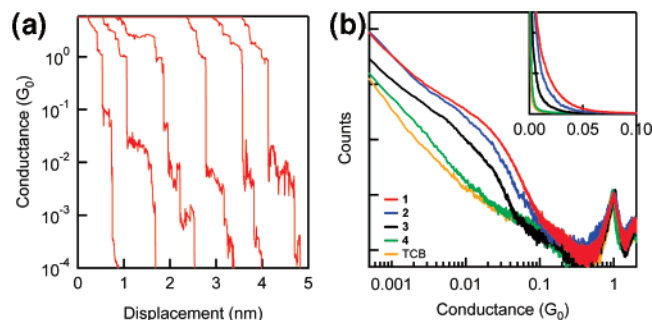


**Figure 2.** (a) Sample breaking conductance trace measured in the presence of compound **1** at an applied bias voltage of 25 mV and a pulling rate of 20 nm/s. Traces show noisy steplike features occurring over a range of conductance values below about  $0.1 G_0$ . (b) Conductance histograms of compounds **1**, **2**, **3**, and **4** constructed from 5000 (2000) consecutively measured traces for molecules **1**, **3**, and **4** (**2**) and control histogram in the solvent alone shown on a log–log scale. All histograms are normalized by the number of traces. Inset: The same histograms on a linear scale. The bias voltage is 25 mV, and the histogram bin size is  $10^{-4} G_0$ .

state<sup>29</sup> and **8** has not been structurally characterized. Compounds **5** and **6** have phosphine ligands with intermediate cone angles and were prepared specifically for this study but not structurally characterized.

The method used to form molecular junctions for conductance studies uses a modified scanning tunneling microscopy (STM), was initially developed by Xu and Tao,<sup>9</sup> and has been described in detail elsewhere.<sup>15,30</sup> Briefly, a gold STM tip is brought in and out of contact with a gold substrate in the presence of a solution of the molecules. A constant bias is applied between the tip and the substrate, and the current is monitored during the measurements. The conductance decreases in a stepwise fashion with each step occurring at an integer multiple of the conductance quantum  $G_0 = 2e^2/h$ .

Conductance histograms reveal pronounced peaks near multiples of  $G_0$ . When the single Au atom contact is broken in solutions of molecules **1**, **2**, or **3**, additional steps in individual conductance traces below  $G_0$  can be observed as shown in Figure 2a for molecule **1**. In the presence of molecule **4**, additional steps are rarely seen in the conductance traces. The additional steps seen with molecules **1**, **2**, or **3** are due to the trapping of one or more molecules between the breaking point contacts. In comparison to the conductance steps seen in the presence of diamine molecules,<sup>15,16</sup> these steps are much noisier, indicating a binding geometry that is not well defined. In addition, multiple steps are frequently seen, indicating that as the junction is being pulled, changes in the detailed atomic configurations result in large changes in conductances. Histograms of the conductance traces calculated without any data selection or processing are shown in Figure 2b on a log–log scale along with a histogram measured in the solvent alone. There is a clear increase in the number of counts below  $\sim 0.1 G_0$  for molecules **1** (red), **2** (blue), and **3** (black), when compared to the control histogram (yellow).

For the  $\{(R_3P)Au\}$ -containing molecules, there are two possible mechanisms for the electrode Au atom to bind to the molecule. One is through a Au(electrode)–Au(molecule) link. The potential for a direct gold–gold contact is feasible for the molecules with a small phosphine capping ligand such as  $P(OMe)_3$  (**1**) (and ligands  $PMe_2Ph$  (**5**) and  $PMe_3$  (**7**)) as shown in the Supporting Information). However, in the case of bulkier phosphines such as  $Pcy_3$  (**4**) (and  $PMePh_2$  (**6**) and  $PPh_3$  (**8**), Supporting Information), this is not necessarily the case, hence, the lack of additional steps in the data collected with molecules

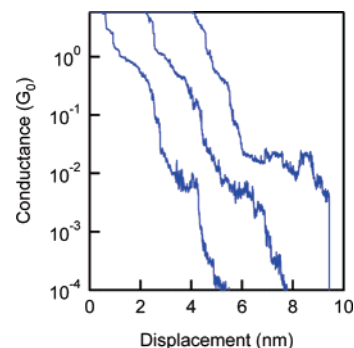


**Figure 3.** Sample conductance trace measured with molecule **2** after collecting over a few thousand traces. The junctions do not show clear steps at integer multiples of  $G_0$ , do not have clean breaks, and extend much longer than those shown in Figure 2a. Data collected with an applied bias of 25 mV at a pulling rate of 20 nm/s.

**4**, **6**, and **8**. The second possible binding geometry is through the formation of molecular junctions with direct Au(electrode)–C link. Although we cannot conclude definitively on the binding mode, the latter case is more likely given the fact that conductance histograms in the presence of molecules **2**, **3**, and **5** reveal additional steps. In this case, the role of the  $\{(R_3P)Au\}$  capping units could be to provide a more chemically robust terminal group ( $R_3P$ ) than the hydrogen atom of **1**, and the Au atom acts as a spacer to permit steric access of the STM tip and surface to the acetylene groups that is not present in **3**.

Further insight can be gained from the conductance histograms of the protonated version of the linker, molecule **2**. Initial traces (around 2000) in a solution of molecule **2** show similar conductance behavior to that of compound **1** (Figure 2). After the initial  $\sim 2000$  scans, the region around the STM tip gets covered with a polymer-like material preventing further measurements and conductance traces often do not break within a 10 nm extension and do not show clear steps at integer multiples of  $G_0$  (sample traces shown in Figure 3). We propose that this polymerization is due to deprotonation of the ethynyl groups and hydrogen atom radical formation by a reactive atomic-gold site, such as an adatom<sup>15</sup>, on an electrode surface. It is plausible that upon radical formation dimers, trimers, and longer oligomers of phenylacetylene are readily formed between the tip and substrate. When oligomerization of the organic units exceeds the solubility limit, conductances can no longer be measured. Gold thiols achieve their robust binding to gold through similar activation of a terminal H–S bond. The polymerization of molecule **2** in our system probably follows either electrochemical or thermal radical polymerization, based on previously reported polymerization studies by Akagi and Shirakawa<sup>31</sup> and Oancea et al.,<sup>32</sup> respectively. Cyclic voltammetry and UV–vis studies were carried out on solutions of molecule **2** in 1,2,4-trichlorobenzene (TCB) which support this hypothesis and can be seen in the Supporting Information.

The triply bonded acetylene groups have high electron density and side-on bonding of gold to acetylene units has been well-characterized by infrared spectroscopy in the solid state.<sup>20,33</sup> Bonding of the STM tip and surface to the Au atom in the molecule would create a  $Au-(Au-C_{10}H_4-Au)-Au$  path of conductance, whereas contact through the acetylene group would create a  $Au-(C_{10}H_4)-Au$  path. These two possibilities are not distinguishable in the experimental data on the  $R_3PAu-C_{10}H_4-AuPR_3$  compounds. A conducting contact through the central arene ring is unlikely given that the arene solvent shows no significant conductance. The conductance measured in repeated junctions varies considerably from junction to junction, sug-



gesting significant variance in the geometric details of the junction. The high conductance tails for **1**, **2**, and **3** exceed that of the diamino-alkanes and 1,4-diamino-benzene<sup>15</sup> implying that in the highest conducting geometry, transport could be outside the nonresonant tunneling regime.

### Experimental Details

The syntheses of compounds **1**, **4**, **7**, and **8** have been previously reported by Millar et al.,<sup>27</sup> Jia et al.,<sup>20</sup> Hurst et al.,<sup>34</sup> and Chao et al.,<sup>29</sup> respectively. Compounds **2** and **3** are commercially available. All syntheses were carried out in an anhydrous dinitrogen atmosphere, and all solvents used were dried to less than 0.1 ppm of H<sub>2</sub>O using standard drybox or Schlenk-line techniques. The solvent (TCB) was purchased from Sigma-Aldrich and used after purification via vacuum distillation from CaH<sub>2</sub>. The coordination polymer {(AuC≡C)<sub>2</sub>p-C<sub>6</sub>H<sub>4</sub>}<sub>n</sub> was prepared by modification of a method reported by Jia et al.<sup>20</sup>

**$\mu$ -p-Phenylenediethynyl-bis[(dimethylphenyl Phosphine)-gold(I)], **5**.** The P(Me)<sub>2</sub>Ph ligand (Aldrich, 0.107 g, 0.77 mmol) was added to a slurry of the polymer {(AuC≡C)<sub>2</sub>p-C<sub>6</sub>H<sub>4</sub>}<sub>n</sub> (0.200 g, 0.385 mmol) in CH<sub>2</sub>Cl<sub>2</sub> causing the polymer to dissolve as the phosphine broke up the intermolecular gold–acetylene interactions. The solution was filtered and layered with hexanes to afford **3**, as a yellow powder. After three successive recrystallizations from CH<sub>2</sub>Cl<sub>2</sub>/hexanes, analytically pure, yellow/amber-colored crystals were obtained (0.242 g, 79% yield). <sup>1</sup>H NMR (300 MHz, CDCl<sub>3</sub>):  $\delta$  1.58 (d, 12H, CH<sub>3</sub>, <sup>2</sup>J<sub>HC</sub> = 19.55 Hz), 7.37 (s, 4H, C<sub>6</sub>H<sub>4</sub>), 7.51 (m, 6H, {*m* and *p*}-C<sub>6</sub>H<sub>5</sub>), 7.76 (m, 4H, {*o*}-C<sub>6</sub>H<sub>5</sub>). <sup>31</sup>P NMR (121 MHz, CDCl<sub>3</sub>):  $\delta$  11.34 (P(Me)<sub>2</sub>Ph). UV–vis (CH<sub>2</sub>Cl<sub>2</sub>) [ $\lambda_{\text{max}}$ , nm ( $\epsilon$ , cm<sup>−1</sup> M<sup>−1</sup>): 228 (158 000), 287 (92 000), 305 (191 000), 325 (251 000). Anal. Calcd for C<sub>26</sub>H<sub>26</sub>Au<sub>2</sub>P<sub>2</sub>: C, 39.31; H, 3.30%. Found: C, 39.12; H, 3.38%.

**$\mu$ -p-Phenylenediethynyl-bis[(diphenylmethyl Phosphine)-gold(I)], **6**.** The PMe(Ph)<sub>2</sub> ligand (Aldrich, 0.155 g, 0.77 mmol) was added to a slurry of the polymer {(AuC≡C)<sub>2</sub>p-C<sub>6</sub>H<sub>4</sub>}<sub>n</sub> (0.200 g, 0.385 mmol) in CH<sub>2</sub>Cl<sub>2</sub> causing the polymer to dissolve. The solution was filtered and layered with hexanes to afford **4**, as a white/yellow powder. After three successive recrystallizations from CH<sub>2</sub>Cl<sub>2</sub>/hexanes, analytically pure, yellow-colored crystallites were obtained (0.189 g, 54% yield). <sup>1</sup>H NMR (300 MHz, CDCl<sub>3</sub>):  $\delta$  2.08 (d, 6H, CH<sub>3</sub>, <sup>2</sup>J<sub>HC</sub> = 20.10 Hz), 7.38 (s, 4H, C<sub>6</sub>H<sub>4</sub>), 7.45 (m, 12H, {*m* and *p*}-C<sub>6</sub>H<sub>5</sub>), 7.62 (m, 8H, {*o*}-C<sub>6</sub>H<sub>5</sub>). <sup>31</sup>P NMR (121 MHz, CDCl<sub>3</sub>):  $\delta$  23.98 (PMe(Ph)<sub>2</sub>). UV–vis (CH<sub>2</sub>Cl<sub>2</sub>) [ $\lambda_{\text{max}}$ , nm ( $\epsilon$ , cm<sup>−1</sup> M<sup>−1</sup>): 290 (50 000), 305 (110 000), 325 (156 000). Anal. Calcd for C<sub>36</sub>H<sub>30</sub>Au<sub>2</sub>P<sub>2</sub>: C, 47.07; H, 3.29%. Found: C, 47.21; H, 3.22%.

### Conclusions

Conductance traces were recorded for solutions of molecules containing the  $\mu$ -p-phenylenediethynyl X–C≡C–C<sub>6</sub>H<sub>4</sub>–C≡C–X unit, containing capping {(R<sub>3</sub>P)Au}, SiMe<sub>3</sub>, and H groups. The traces collected in the presence of molecules with smaller capping groups reveal additional steps at conductances as high as 0.1 G<sub>0</sub> (G<sub>0</sub> = 2e<sup>2</sup>/h) down to the measurable limits of the experimental setup. The X–C≡C–C<sub>6</sub>H<sub>4</sub>–C≡C–X unit does not show a discrete conductance value but does exhibit relatively high conductances for a large number of transients in compounds **1**, **2**, **3**, **5**, and **7**. These results suggest that a strong, directional bond is required to form a narrow range of molecule–electrode contact geometries and lead to peaks in conductance histograms. Although the {Au–C<sub>10</sub>H<sub>4</sub>–Au} unit is attractive as a potential molecular electronics component with the ability to make

metal–electrode contacts and utilize the delocalized  $\pi$ -system, its discrete conductance cannot be measured by this technique. The ideal molecular wire will provide (i) a chemically robust bond to the electrode with limited atomic-scale rearrangements, (ii) similar orbital energy overlap between atoms in the molecule and atoms in the contact, and (iii) facile electronic conduction through a delocalized  $\pi$ -system. The challenge of preparing and characterizing such a system remains.

**Acknowledgment.** This work was supported by an NSF-CAREER Award (to L.H.D.; Grant No. CHE-0134817) and partially funded by the Nanoscale Science and Engineering Initiative of the National Science Foundation under NSF Award No. CHE-0117752 and by the New York State office of Science, Technology and Academic Research (NYSTAR). We thank M. S. Hybertsen for thoughtful discussions.

**Supporting Information Available:** Conductance histograms of L–Au–C<sub>10</sub>H<sub>4</sub>–Au–L (L = PMe<sub>3</sub> (**7**), PMe<sub>2</sub>Ph (**5**), PMePh<sub>2</sub>(**6**), Pcy<sub>3</sub> (**4**)) with similar geometries and chemical structures also studied (Figure S1), UV–vis spectra of molecule **1** in TCB solution in the presence and absence of gold and with heating to 50 °C (Figure S2), cyclic voltammograms of molecule **1** in TCB under oxidizing and reducing potentials (Figure S3). This material is available free of charge via the Internet at <http://pubs.acs.org>.

### References and Notes

- Gimzewski, J. K.; Joachim, C. *Science* **1999**, *283*, 1683–1688.
- Joachim, C.; Gimzewski, J. K.; Aviram, A. *Nature* **2000**, *408*, 541–548.
- Reed, M. A.; Zhou, C.; Muller, C. J.; Burgin, T. P.; Tour, J. M. *Science* **1997**, *278*, 252–254.
- Cui, X. D.; Primak, A.; Zarate, X.; Tomfohr, J.; Sankey, O. F.; Moore, A. L.; Moore, T. A.; Gust, D.; Harris, G.; Lindsay, S. M. *Science* **2001**, *294*, 571–574.
- Kushmerick, J. G.; Holt, D. B.; Pollack, S. K.; Ratner, M. A.; Yang, J. C.; Schull, T. L.; Naciri, J.; Moore, M. H.; Shashidhar, R. *J. Am. Chem. Soc.* **2002**, *124*, 10654–10655.
- Park, J.; Pasupathy, A. N.; Goldsmith, J. I.; Chang, C.; Yaish, Y.; Petta, J. R.; Rinkoski, M.; Sethna, J. P.; Abruna, H. D.; McEuen, P. L.; Ralph, D. C. *Nature* **2002**, *417*, 722–725.
- Reichert, J.; Ochs, R.; Beckmann, D.; Weber, H. B.; Mayor, M.; Lohneysen, H. V. *Phys. Rev. Lett.* **2002**, *88*, 176804–1–176804–4.
- Liang, W.; Shores, M. P.; Bockrath, M.; Long, J. R.; Park, H. *Nature* **2002**, *417*, 725–729.
- Xu, B.; Tao, N. J. *Science* **2003**, *301*, 1221–1223.
- Bott, R. C.; Healy, P. C.; Smith, G. *Aust. J. Chem.* **2004**, *57*, 213–218.
- Fishelson, N.; Shkrob, I.; Lev, O.; Gun, J.; Modestov, A. D. *Langmuir* **2001**, *17*, 403–412.
- Blum, A. S.; Kushmerick, J. G.; Pollack, S. K.; Yang, J. C.; Moore, M.; Naciri, J.; Shashidhar, R.; Ratna, B. R. *J. Phys. Chem. B* **2004**, *108*, 18124–18128.
- Dadosh, T.; Gordin, Y.; Krahne, R.; Khivrich, I.; Mahalu, D.; Frydman, V.; Sperling, J.; Yacoby, A.; Bar-Joseph, I. *Nature* **2005**, *436*, 677–680.
- Tivanski, A. V.; He, Y.; Borguet, E.; Liu, H.; Walker, G. C.; Waldeck, D. H. *J. Phys. Chem. B* **2005**, *109*, 5398–5402.
- Venkataraman, L.; Klare, J. E.; Tam, I. W.; Nuckolls, C.; Hybertsen, M. S.; Steigerwald, M. L. *Nano Lett.* **2006**, *6*, 458–462.
- Venkataraman, L.; Klare, J. E.; Nuckolls, C.; Hybertsen, M. S.; Steigerwald, M. L. *Nature* **2006**, *442*, 904–907.
- Xue, Y.; Datta, S.; Ratner, M. A. *J. Chem. Phys.* **2001**, *115*, 4292–4299.
- Tulevski, G. S.; Myers, M. B.; Hybertsen, M. S.; Steigerwald, M. L.; Nuckolls, C. *Science* **2005**, *309*, 591–594.
- Siaj, M.; McBreen, P. H. *Science* **2005**, *309*, 588–590.
- Jia, G.; Puddephatt, R. J.; Scott, J. D.; Vittal, J. J. *Organometallics* **1993**, *12*, 3565–3574.
- MacDiarmid, A. G. *Angew. Chem., Int. Ed.* **2001**, *40*, 2581–2590.
- Nitzan, A.; Ratner, M. A. *Science* **2003**, *300*, 1384–1389.
- Bondi, A. J. *Phys. Chem.* **1966**, *70*, 3006–3007.

- (24) Pyykkö, P. *Chem. Rev.* **1997**, 97, 597–636.
- (25) Schneider, W.; Bauer, A.; Schmidbaur, H. *Organometallics* **1996**, 15, 5445–5446.
- (26) Hollatz, C.; Schier, A.; Schmidbaur, H. *J. Am. Chem. Soc.* **1997**, 119, 8115–8116.
- (27) Millar, D.; Zakharov, L. N.; Rheingold, A. L.; Doerr, L. H. *Acta Crystallogr., Sect. C: Cryst. Struct. Commun.* **2005**, C61, m90–m92.
- (28) Tolman, C. A. *Chem. Rev.* **1977**, 77, 313–348.
- (29) Chao, H.-Y.; Lu, W.; Li, Y.; Chan, M. C. W.; Che, C.-M.; Cheung, K.-K.; Zhu, N. *J. Am. Chem. Soc.* **2002**, 124, 14696–14706.
- (30) Ulrich, J.; Esrail, D.; Pontius, W.; Venkataraman, L.; Millar, D.; Doerr, L. H. *J. Phys. Chem. B* **2006**, 110, 2462–2466.
- (31) Akagi, K.; Shirakawa, H. *Plast. Eng.* **1998**, 45, 983–1010.
- (32) Oancea, D.; Schuster, R. H.; Caragheorgheopol, A.; Nicolau, A.; Ionescu, N. I.; Popescu, D. *Plaste Kautsch.* **1979**, 26, 213.
- (33) Yam, V. W.-W.; Choi, S. W.-K. *J. Chem. Soc., Dalton Trans.* **1996**, 4227–4232.
- (34) Hurst, S. K.; Cifuentes, M. P.; McDonagh, A. M.; Humphrey, M. G.; Samoc, M.; Luther-Davies, B.; Asselberghs, I.; Persoons, A. *J. Organomet. Chem.* **2002**, 642, 259–267.